

# A SCANNING MICROMIRROR WITH ANGULAR COMB DRIVE ACTUATION

Pamela R. Patterson, Dooyoung Hah, Hung Nguyen, Hiroshi Toshiyoshi<sup>1</sup>, Ru-min Chao, and Ming C. Wu

Electrical Engineering Department, University of California at Los Angeles  
Los Angeles, California 90095-1594

<sup>1</sup>Institute of Industrial Science, University of Tokyo  
Tokyo 153-8585, Japan

## ABSTRACT

We describe a single crystal silicon,  $1 \times 1 \text{ mm}^2$ , scanning micromirror, which incorporates a novel angular vertical comb drive actuator. Results from our model for the angular vertical comb show that a 50% higher scan angle can be achieved when compared to a staggered vertical comb of equivalent dimensions. The simplified, cost effective, silicon on insulator micro-electro-mechanical systems, (SOI MEMS), process features self-alignment of the fixed and moving teeth and is fabricated on a single SOI wafer. Static deflection for our fabricated device fits well with the model and a resonant mode optical scan angle of  $\pm 18^\circ$  at 1.4 kHz has been measured.

## INTRODUCTION

Micromachining technology enables the creation of miniaturized, light weight, low energy, and reduced cost optical scanners for a wide range of applications including: optical switches, imaging, optical data storage, bar code reading, and beam steering for free-space optical communication. For high speed scanning applications, electrostatic comb drive actuation has several advantages. A relatively stiff torsion bar, required for high frequency operation, may be designed since the increased force generated by the large capacitance area provides more effective utilization of the driving voltage. In addition, decoupling of the mirror and actuator permits a large deflection angle since, the under mirror electrode is not required and the underside can be opened to accommodate a larger range of motion.

Unlike lateral comb drives [1], vertical comb drives require a disruption of the electrostatic field to create a force normal to the comb plane for actuation. Vertical comb drives have been demonstrated, with a staggered vertical comb drive by patterning the fixed and moving teeth in distinct

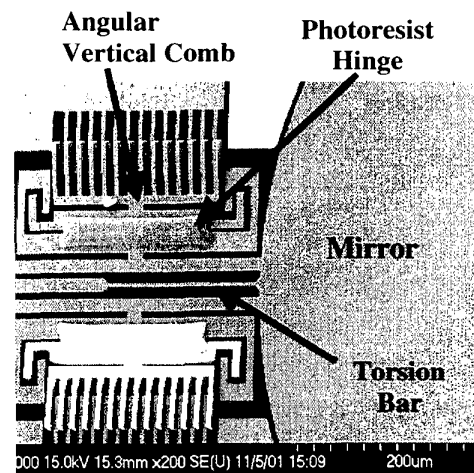


Figure 1. Scanning Electron Micrograph, (SEM), of scanning micromirror with AVC.

layers separated by sacrificial oxide [2], or by adding a metal offset electrode on top of the fixed teeth [3]. The staggered vertical comb drive requires critical alignment, although a self-aligned process was reported very recently [4], where sacrificial comb teeth are used such that the final etch defines both the fixed and moving comb.

Our approach, the angular vertical comb, (AVC) [5], is fabricated from the device layer of a single SOI wafer, Fig. 1. The self-aligned comb fingers are patterned in a single etching process and subsequently rotated out of the wafer plane and therefore, no critical alignment is needed. Furthermore, our model shows that an angular vertical comb can achieve a 50% higher scan angle than a staggered vertical comb of equivalent dimensions.

## THEORY

The vertical comb drive actuators, shown schematically in Fig. 2, can be described as follows. When voltage is applied between the movable and the fixed comb fingers, the movable fingers rotate about the torsion spring axis until the restoring torque and the electrostatic torque are equal.

The torques can be expressed as:

$$T_e(\theta) = \frac{V^2}{2} \frac{\partial C}{\partial \theta} = N_f V^2 \frac{\partial C_{unit}}{\partial \theta} \quad (1)$$

$$T_r(\theta) = \frac{2Gw_s^3 t_s}{3l_s} \left[ 1 - \frac{192}{\pi^5} \frac{w_s}{t_s} \tanh\left(\frac{\pi t_s}{2w_s}\right) \right] \theta \quad (2)$$

where,

$C_{unit}$ : unit capacitance between a fixed and movable tooth

$G$ : shear modulus

$N_f$ : number of teeth

$t_s$  (thickness),  $w_s$  (width),  $l_s$  (length) of spring

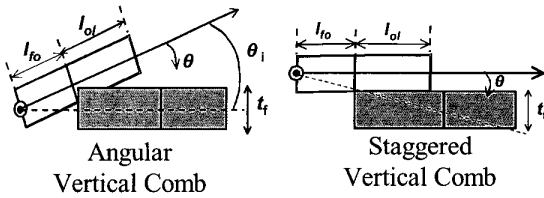


Figure 2. Schematic view of the angular vertical comb, (AVC), and the staggered vertical comb, (SVC), in the initial state.

It can be shown that the maximum scan angle is a function of the finger geometry, specifically the finger thickness, the finger overlap, and the finger offset. Equation (3) shows this relationship for the staggered vertical comb and equation (4) shows the relationship for the angular vertical comb.

$$\theta_{max} = \frac{t_f}{l_{ol} + l_{fo}} \quad (3)$$

$$\theta_{max} = 1.5 \frac{t_f}{l_{ol} + l_{fo}} \quad (4)$$

For both types of combs, the maximum scan angle is limited by the polarity change of the electrostatic force as the top of the moving finger passes below the top of the fixed finger. For the angular vertical comb, however, the larger initial angle increases the angular range. Our model [6], shows that this initial angle, ( $\theta_{max}$ ), is eventually limited by pull in as shown by the analytical solutions in Fig. 3 where pull-in is evident at 40°. Comprehensive analysis

shows that a 50% greater scan angle can be achieved for the angular comb drive (Fig. 4).

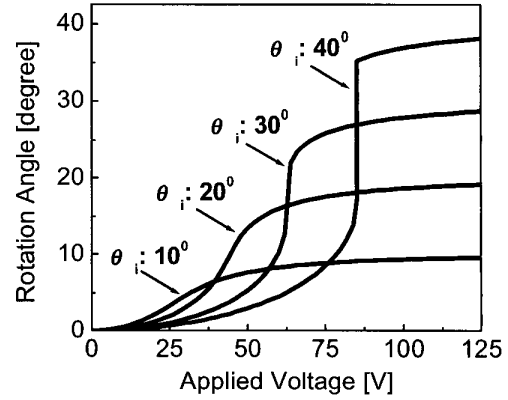


Figure 3. Transfer curves at various initial angles.

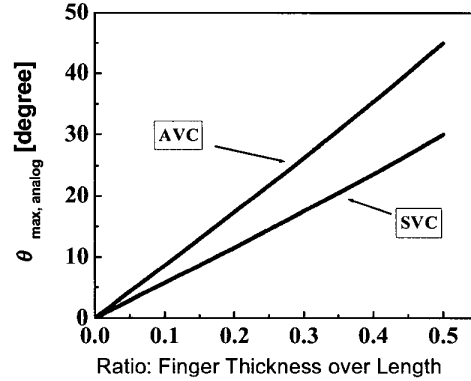


Figure 4. Maximum analog scanning angle of angular vs. staggered comb-drive actuator.

## DESIGN AND FABRICATION

Simplified schematics of two designs for the scanning mirror with the angular vertical comb drive are shown in Fig. 5. The newer, 2<sup>nd</sup>, design was developed to eliminate the transfer of stress from the photoresist hinge to the central axis of the mirror. We experimentally determined that the photoresist hinge caused a sag in our first mirror design from 10 to 20  $\mu\text{m}$ , depending on the length of the torsion bar. Finite element analysis was used to model this downward deflection. An average stress of 12 MPa created by the photoresist was found to provide good agreement between simulated and measured results. In our new design, the mirror sag has been reduced to 0.13  $\mu\text{m}$ .

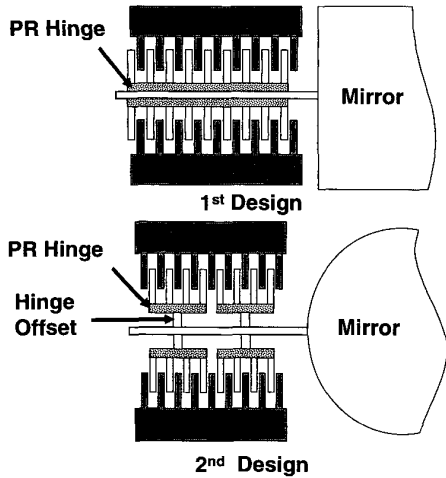


Figure 5. Simplified schematic of 1<sup>st</sup> and 2<sup>nd</sup> design for elimination of stress transfer.

The fabrication process outlined in Fig. 6 is described in detail below. The process begins with an SOI wafer with a top layer of 25  $\mu\text{m}$ , and a substrate, which was lapped down 350  $\mu\text{m}$ . The device layer was etched in a Plasmatherm SLR deep reactive ion etcher utilizing photoresist, AZ5214, as a mask. The minimum line size in the device pattern is 3  $\mu\text{m}$  and the minimum space is 2  $\mu\text{m}$ . An LPCVD oxide of 3  $\mu\text{m}$  was deposited to provide some degree of planarization and mechanical stability to the structure after subsequent backside removal. Next the backside layer was aligned and patterned using the backside alignment feature on a K. Suss MA 6 aligner. The backside substrate was removed under the mirror and comb structures with DRIE and STR-1045 photoresist as an etch mask. Next the deposited oxide was patterned and dry etched in the regions where the hinge photoresist would anchor to the silicon. A thick photoresist, AZ-4620, spun at 1400 rpm, was used to create the hinges and resulted in a final thickness  $\sim 9.5 \mu\text{m}$ . The resist was premelted at 100°C for 30 minutes prior to HF release [7]. The device was released in 49% HF for 20 minutes. After release the samples were placed in DI water at  $\sim 104^\circ\text{C}$  for 2 hours to reflow the resist and assemble the moving teeth. Ceramic chips were used to prevent vigorous boiling. The samples were allowed to air dry after which a blanket metallization of 5nm chromium and 100nm of gold was deposited with an e-beam evaporator. The final device is shown in the SEM images of Fig. 7. Etching of the backside after the

etch step of the LPCVD oxide was found to attack the top silicon layer in some areas. To prevent this, the order of the two etches was reversed so that the topside was completely protected by LPCVD oxide during backside silicon etching. Optimization of the process to improve the planarity of the top layer is ongoing as photoresist residue in high aspect ratio features impacts the device yield during hinge patterning.

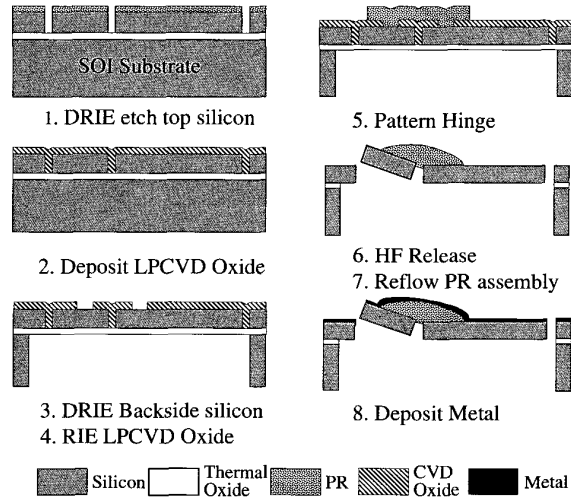


Figure 6. Fabrication Process Flow

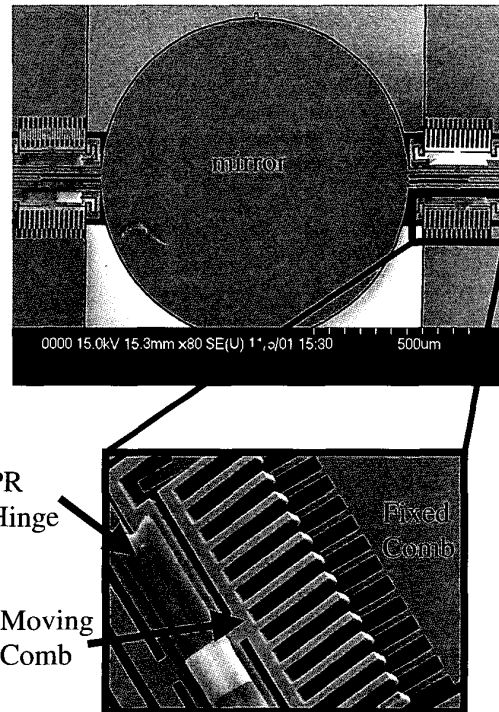


Figure 7. SEM of scanner with angular vertical comb drive, inset comb teeth.

## RESULTS AND DISCUSSION

The resonant frequency for the scanning micromirrors was characterized with a Polytech Vibscan laser doppler vibrometer. A resonant frequency of 1.4 kHz was measured for the device which is in good agreement with the calculated value of 1.44 kHz. The transfer curve for the device is shown in Fig. 8, and was found by measuring the static deflection, as a function of DC voltage, with a Wyko RTS 500 surface profiler. The measured data points fit well with the numerical solution derived from our model shown by the solid curve.

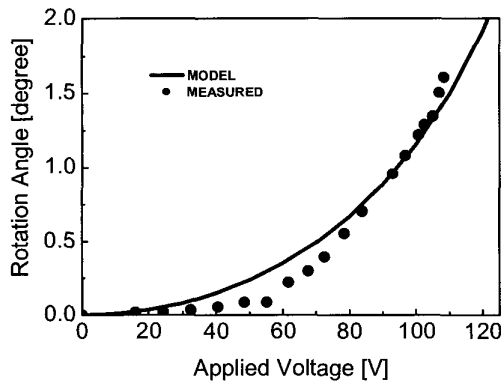


Figure 8. DC transfer curve

As stated previously, the maximum scan angle for the angular vertical comb is determined by the geometry of the comb. The measured device has 40 fingers with 40  $\mu\text{m}$  overlap length and a gap spacing of 3  $\mu\text{m}$ . The design space depicted in Fig. 9, shows that by increasing the finger length and the number of fingers we can achieve scan angles  $> 10^\circ$  at 100V. The finger thickness for all curves is 25  $\mu\text{m}$ , by increasing the comb finger thickness to 50  $\mu\text{m}$  or more, the voltage can be further reduced. Deflection at resonance is significantly larger and we have measured an optical scan angle of  $\pm 18^\circ$  with a 21V sinusoidal input at 1.4 kHz.

## CONCLUSION

We have demonstrated a scanning micromirror actuated with our new angular vertical comb drive. The scanner was fabricated using a self-aligned process on a single SOI wafer and a resonant mode scan angle of  $\pm 18^\circ$  at 21V has been achieved for the device at 1.4 kHz.

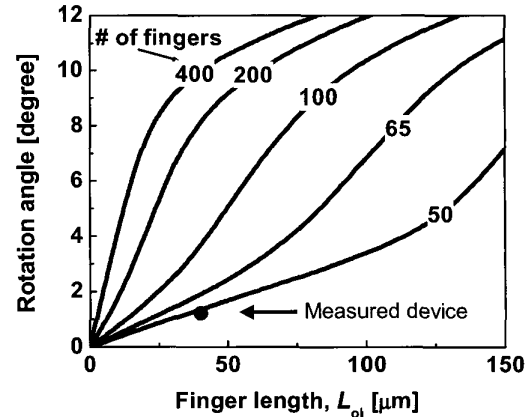


Figure 9. Scan angle vs. finger length and number for angular vertical comb drive at 100V applied voltage.

## ACKNOWLEDGEMENTS

The authors would like to thank Tom Lee, Wibool Piyawattanametha, and Henry Yang for technical assistance. This project is supported by DARPA.

## REFERENCES

1. V. Milanovic, M. Last, K.S.J.Pister, "Torsional Micromirrors with Lateral Actuators" Transducers 01, Munich, Germany, pp.1290-1301.
2. R. A. Conant, J.T. Nee, K. Lau, R.S. Mueller "A Flat High-Frequency Scanning Micromirror", 2000 Solid-State Sensor and Actuator Workshop, Hilton Head, SC, pp. 6-9.
3. H. Schenk, P.Dürr, T. Hasse, D. Kunze, U. Sobe, H.Kück, "Large Deflection Micromechanical Scanning Mirrors for Linear Scans and Pattern Generation", IEEE Journal of Selected Topics in Quantum Electronics, vol. 6, no.5, Sept./Oct. 2000, pp.715-722.
4. U. Krisnamoorthy and O. Solgaard, "Self-aligned Vertical Comdrive Actuators for Optical Scanning Micromirrors" 2001 International Conference on Optical MEMS, Okinawa, Japan,p.41.
5. P. Patterson, D. Hah, H. Chang, H. Toshiyoshi, M.C. Wu, "An Angular Vertical Comb Drive Actuator for Scanning Micromirrors", 2001 International Conference on Optical MEMS, Okinawa, Japan,p.25.
6. D. Hah, H. Toshiyoshi, and M.C. Wu, "Design of Electrostatic Actuators for MOEMS", submitted to Symposium on Design, Test, Integration and Packing of MEMS/MOEMS 2002.
7. R.R.A. Syms, C. Gormley, S. Blackstone,"Improving Yield, Accuracy and Complexity in Surface Tension Self-Assembled MOEMS", Sensors and Actuators A 88 (2001) 273-283.